Developmental Cell
Article

Zona Pellucida Domain Proteins Remodel the Apical Compartment for Localized Cell Shape Changes

Isabelle Fernandes,[1,2,4] Hélène Chanut-Delalande,[1,2,4] Pierre Ferrer,[1,2] Yvan Latapie,[1,2] Lucas Waltzer,[1,2] Markus Affolter,[3] François Payre,[1,2,*] and Serge Plaza[1,2,*]
[1]Université de Toulouse, UPS; Centre de Biologie du Développement; F-31062, Toulouse, France
[2]CNRS, UMR5547, Centre de Biologie du Développement, F-31062, Toulouse, France
[3]Biozentrum der Universität Basel, 4056 Basel, Switzerland
[4]These authors contributed equally to the work
*Correspondence: payre@cict.fr (F.P.), plaza@cict.fr (S.P.)
DOI 10.1016/j.devcel.2009.11.009

SUMMARY

The zona pellucida domain (ZPD) defines a conserved family of membrane-anchored matrix proteins that are, as yet, poorly characterized with respect to their functions during development. Using genetic approaches in flies, we show here that a set of eight ZPD proteins is required for the localized reorganization of embryonic epidermal cells during morphogenesis. Despite varying degrees of sequence conservation, these ZPD proteins exert specific and nonredundant functions in the remodeling of epidermal cell shape. Each one accumulates in a restricted subregion of the apical compartment, where it organizes local interactions between the membrane and the extracellular matrix. In addition, ZPD proteins are required to sculpture the actin-rich cell extensions and maintain appropriate organization of the apical compartment. These results on ZPD proteins therefore reveal a functional subcompartmentalization of the apical membrane and its role in the polarized control of epithelial cell shape during development.

INTRODUCTION

Recent studies have demonstrated the importance of variations in the apical area of epithelial cells for the morphogenesis of different tissues (Lecuit and Lenne, 2007). However, the mechanisms by which terminal differentiation produces highly ordered three-dimensional structures within the apical compartment remain poorly understood. In many cases, specific membrane extensions are required for the function of epithelial cells, and human diseases, such as deafness or retinal disorders, are linked to improper morphological differentiation of corresponding cells. Deciphering the dynamic networks that remodel the shape of epithelial cells is thus a prerequisite to understanding normal morphogenesis of animal cells, as well as various pathological states.

A primary step for the localized remodeling of epithelial cells is their polarization along the apical-basal axis. According to current models (Wodarz and Nathke, 2007), three main processes interact to modify the basic cellular mechanisms and lead to the polarized distribution of various molecules (Mellman and Nelson, 2008). First, posttranslational control of protein sorting and intracellular trafficking provides intrinsic cues for the localized delivery of membrane components. Second, together with the cytoskeleton, protein complexes act as polarity determinants to provide orientation cues that specify overall cell polarity and shape (Wodarz and Nathke, 2007). Finally, extracellular cues are required to orientate intracellular mechanisms into a topologically ordered three-dimensional space (Schock and Perrimon, 2002). It is well documented that adhesion, both between cells and between cells and the basal extracellular matrix (ECM), provides extrinsic information for changes in cell shape. In striking contrast, little is known about a putative influence of the apical ECM (aECM) on the control of epithelial cell organization.

Drosophila embryonic epidermal cells are highly polarized and secrete proteins and polysaccharides that form a prominent aECM, known as cuticle, which protects the animal against the external milieu (Locke, 2001; Payre, 2004). The epidermis is composed of a monolayer of cells that adopt two distinct morphologies: (1) smooth cells and (2) cells producing actin-rich apical extensions, called denticles, in the ventral region and hairs in the dorsal region (collectively referred to as trichomes). The pattern of trichomes is stereotyped in *Drosophila melanogaster* and displays a wide range of evolutionary diversification between insect species (Delon and Payre, 2004). Results both from developmental and evolutionary studies have shown the importance of the gene *shavenbaby* (*svb*) in determining the trichome pattern (Delon and Payre, 2004; McGregor et al., 2007; Payre et al., 1999; Sucena et al., 2003). The control regions of *svb* integrate multiple inputs, emanating from signaling and positional information, to define the subset of cells forming trichomes in a given species (Delon and Payre, 2004; McGregor et al., 2007; Payre et al., 1999). *Svb* encodes a transcription factor that acts in a cell-autonomous manner to trigger trichome formation (Andrews et al., 2000; Delon et al., 2003), and identification of *svb* downstream targets has provided an unbiased means of discovering direct effectors of epidermal cell remodeling. Svb triggers the expression of regulators of general machineries, such as the ARP2/3 nucleation complex, for the localized polymerization and organization of actin filaments (Chanut-Delalande et al., 2006). More unexpectedly, Svb controls the

expression of cuticle proteins (Andrew and Baker, 2008) and enzymes that increase trichome pigmentation and hardness (Chanut-Delalande et al., 2006). Furthermore, Svb directly controls the transcription of *miniature*, a gene encoding a membrane-anchored extracellular protein required for correct morphogenesis of trichome cells (Chanut-Delalande et al., 2006). These data thus suggest that the morphological differentiation of epidermal cells requires an intimate interaction between polarized actin cytoskeleton and aECM components.

Miniature belongs to a conserved family of aECM proteins, initially identified in the zona pellucida (ZP) coat surrounding mammalian oocytes (reviewed by Jovine et al., 2005). These proteins are characterized by an extracellular motif of 260 aa, the ZP domain (ZPD), the structure of which includes a conserved array of disulfide bridges. The ZPD is thought to act as a polymerization module, promoting the formation of homo- or heterotypic filaments (Jovine et al., 2002). Indeed, the function of ZPD-containing proteins often relies on polymers composed of distinct members of this family. In vertebrates, the heteroassociation of ZP1, -2, and -3 in the ZP coat, and that of α- and β-tectorin in the tectorial membrane, is required for their function (i.e., fertilization and hearing, respectively) (Jovine et al., 2005; Verhoeven et al., 1998). In flies, genetic data also support a concerted action of *piopio* and *dumpy* during tracheal development (Jazwinska et al., 2003), and *miniature* and *dusky* during wing development (Roch et al., 2003).

To explore a possible contribution of multiple ZPD proteins to epidermal morphogenesis, we analyzed the entire ZPD gene family in *Drosophila*. We show that eight ZPD genes are coexpressed in denticle cells, under the transcriptional control of Shavenbaby. Individual ZPD proteins accumulate in separate regions along the cell extension, revealing a subcompartmentalization of the apical region. Ultrastructural analyses show that the lack of each ZPD protein induces specific defects in membrane/aECM interactions in corresponding apical subregions. These results reveal the existence of an ordered assemblage of distinct ZPD proteins, linking the aECM to actin organization and polarity complexes in order to remodel the apical region of epidermal cells.

RESULTS

Diverse Subtypes of ZP Proteins Are Coexpressed in the Epidermis

The *Drosophila* genome encodes 16 proteins with a full-length ZPD and other characteristics of ZPD proteins (Jazwinska and Affolter, 2004), *i.e.*, a peptide signal, a single-pass transmembrane domain and a short C-terminal cytoplasmic tail (Figure 1A). Phylogenetic analyses suggest early separation of most extant *Drosophila* ZPD proteins and underline the existence of additional extracellular domains (Figure 1A). For instance, Dumpy, a giant protein, contains 256 EGF motifs; six ZPD proteins contain 2-4 repeats of the PlAsminogen N terminus (PAN) domain, a cysteine-rich motif involved in protein interactions (Tordai et al., 1999). Although PAN or ZPD are found separately in various animal proteins, the combination of these two motifs in the same protein was not detected in vertebrates (see Table S1 available online). In contrast, we identified PAN-ZPD proteins in arthropods and nematodes, suggesting that they may be specific to ecdysozoan species. In mammals, the number of disulfide bridges defines two sub-types of ZPD domains, possibly related to different functions, with 10 cysteines in ZP1/2 and 8 cysteines in ZP3 (Jovine et al., 2005) (Figure 1B). Both ZP1/2- and ZP3-like ZPDs are found in *Drosophila* proteins, associated with, or independent of, PAN domains (Figures 1A and 1B).

The fact that ZPD proteins generally act within heterotypic polymers suggests that additional ZPD proteins contribute, together with Miniature, to epidermis differentiation. To explore this hypothesis, we systematically analyzed the expression of ZPD genes in trichome cells. Of the ZPD genes expressed in epidermal derivatives (Jazwinska and Affolter, 2004), we found that seven were coexpressed with *m* in trichome cells. We named these putative components of the matrix after characters of the eponymous movie (see Figure 1A). The patterns of expression of *trynity* (*tyn*), *neyo* (*neo*), *morfeyus* (*mey*), *nyobe* (*nyo*), and *dusky-like* (*dyl*) strikingly resembled that of *m* (Figure 1C). Double-staining experiments confirmed that all six ZPD genes were coexpressed in trichome cells, in coinciding time windows (see below). Each of these genes appeared to be transcribed in all trichome cells, with no detectable difference in expression levels. Two additional ZPD genes displayed overlapping but distinct transcription patterns. *zye* expression started later, and was detected only in trichome cells of the ventral region (Figure 1C). *cypher* (*cyr*) displayed a dynamic pattern of expression in trichome cells: *cyr* mRNA was first restricted to dorsal cells (Figure 1C), then it shut down dorsally and was eventually detected only in ventral cells (not shown). As the expression of these ZPD genes strikingly matches the trichome pattern that is specified by *svb*, we examined their dependence on *svb* activity. We found that epidermal expression of each of the eight ZPD genes was abolished or severely reduced in *svb* mutant embryos (Figure 1C). Hence, these results show that *svb* controls the expression of a large and diverse subfamily of ZPD genes in trichome cells.

Each ZPD Protein Exerts a Specific Function in Denticle Cells

The coregulation of ZPD genes in trichome cells suggests that they act with *m* in the formation of apical extensions. To investigate the putative role of ZPD genes in epidermal morphogenesis, we analyzed the consequences of their inactivation.

Notwithstanding morphological features specific to each row, all wild-type denticles share a common organization: a large base, followed by a median constriction supporting the distal hook, which points anteriorly or posteriorly (Figure 2A). We used strong hypomorph alleles of *m*, *tyn*, or *zye*, and generated small deficiencies deleting each of the *neo*, *nyo*, *mey*, *tyn*, *zye*, and *dyl* genes (Figure S1). In all ZPD mutants examined, each denticle row was present, but the denticles themselves displayed an altered morphology (Figure 2A). Re-expression of M, Dyl, Tyn, Neo, Nyo, and Zye in respective mutants restored wild-type denticle shape (Figure 2; Table S2). This indicates that denticle defects result from the lack of each ZPD protein; a weak effect of neighboring genes that are also affected in some deficiencies (Figure S1) cannot be formally ruled out. In the absence of M, denticles were small and lacked the median constriction, adopting an abnormal triangular shape (Figure 2A).

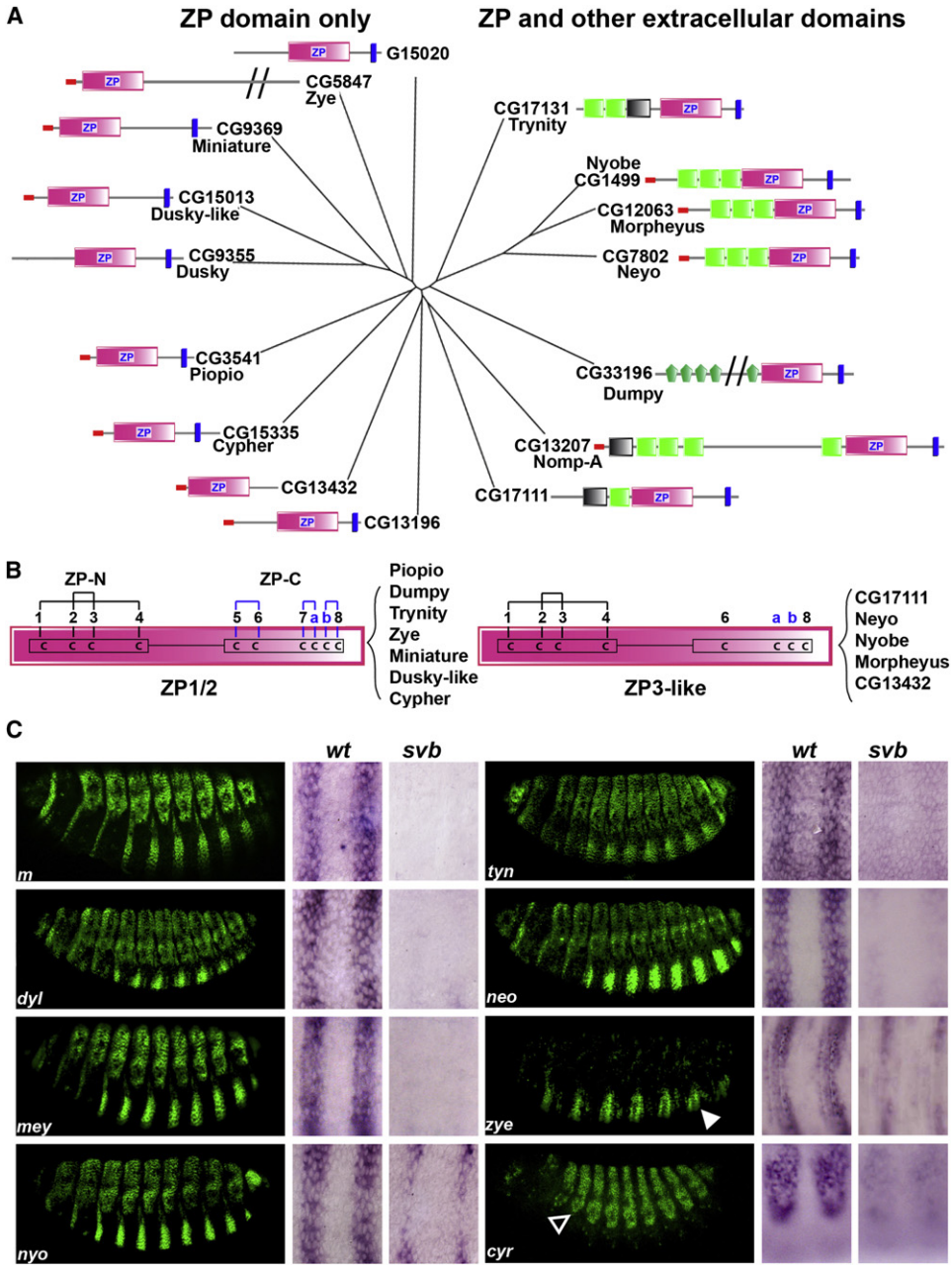

Figure 1. Structure and Expression of *Drosophila* ZPD Proteins

(A) Phylogenetic tree grouping *Drosophila* ZPD proteins according to the conservation of their ZPD (pink rectangle). Seven proteins comprise additional motifs in the extracellular region, such as EGF (green pentagon) or PAN (green and gray boxes) repeats. Signal peptides are drawn in orange and transmembrane domains in blue (see also Table S1).

(B) Patterns of conserved Cys in the ZPD define two subgroups of *Drosophila* proteins, which, like mammalian ZP1/2 and ZP3, contain 10 and 8 residues, respectively.

(C) mRNA expression of *miniature* (*m*), *dusky-like* (*dyl*), *morpheyus* (*mey*), *nyobe* (*nyo*), *trynity* (*tyn*), *neyo* (*neo*), and *cypher* (*cyr*) at stage 15 and *zye* at stage 16. Whole mounts show in situ hybridization in wild-type embryos. Note the expression of *zye* only in the ventral region (closed arrowhead). *Cyr* mRNA is restricted to dorsal cells at stage 15 (open arrowhead), then switches to ventral stripes at stage 16/17. Close-up of ZPD expression in A3-4 abdominal segments in wild-type (*wt*) and *shavenbaby* (*svb*) mutant embryos. All views are of ventral cells, except for *cyr* pictures, showing laterodorsal cells.

dyl mutants were characterized by very small, unhooked denticles, often with a split extremity. Inactivation of *tyn* led to denticles with a flattened base and thin extensions, pointing perpendicularly to the apical surface. The denticles of *zye* mutants were thin and often twisted or broken. While inactivation of *neo* did not affect the overall morphology of denticles, it did lead to a marked decrease in their size. Similarly, *nyo* and *mey* mutants displayed smaller denticles, without other obvious morphological defects.

A

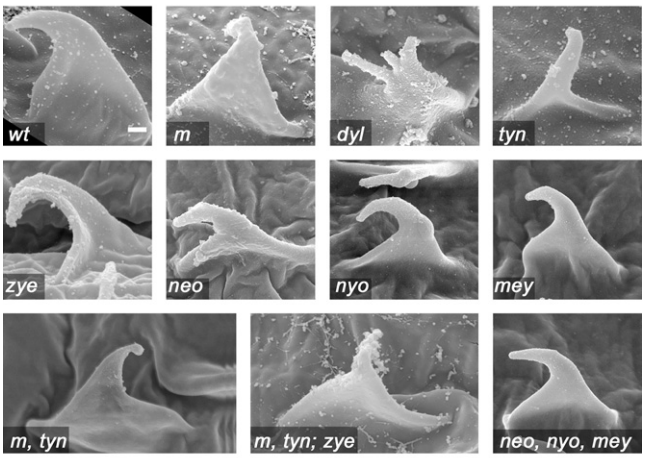

B

	m mutants		*tyn* mutants	
	Denticles	Wings	Denticles	Viability
UAS-*m*	+++	90% +/-7%	-	0%
UAS-*dyl*	+/-	10% +/-4%	-	0%
UAS-*tyn*	-	6% +/-5%	+++	80%
UAS-*neo*	-	3% +/-5%	+	13%
UAS-*nyo*	-	4% +/-4%	+	14%
UAS-*zye*	-	3% +/-5%	-	0%

Figure 2. ZPD Mutants Display Specific Defects in Epidermal Cell Shape

(A) Electron micrographs of denticles (fourth row of the A4 segment). When compared to wild-type, embryos mutant for any ZPD gene (i.e., m^1, $dyl^{\Delta 26}$, zye^{ex72}, tyn^{PG38}, $neo^{\Delta 32}$, $nyo^{\Delta 33}$, or $mey^{\Delta 13}$) display specific alterations of denticle shape. Embryos carrying simultaneous mutations for m^1, tyn^{PG38}, and m^1, tyn^{PG38}, and zye^{ex72} exhibit additive denticle phenotypes, while the combination of $neo^{\Delta 32}$ and *nyo*, *mey* mutations leads to a phenotype similar to that of single mutant. Scale bar, 500 nm (see also Figure S1).

(B) Ability of UAS-cDNA constructs to rescue m^1 and tyn^{PG38} mutant phenotypes, as assayed in embryos (denticles) and adults (wing size or viability, respectively), when expressed using the *da*-GAL4 driver. Symbols: "+++," a full rescue of denticle defects; "+," very partial phenotypical amelioration; "+/−," a slight modification of the denticle phenotype that cannot unambiguously be interpreted as rescuing toward wild-type; and "−," no rescue. Levels of wing size were calculated from 100% rescue (wild-type size) to 0% (size of m^1 mutant wings) (see also Table S2). Adult wings size was determined from measures done with 15–25 wings for each genotype. Average values with SD are indicated. See Supplemental Information for additional information.

We then analyzed embryos carrying combinations of mutations (Figure 2A). The phenotype of *m*, *tyn* double mutants, was aggravated compared to each single mutant. Denticles displayed both the thin extremity found in *tyn* and the lack of medial constriction characteristic of *m* mutants. The additional inactivation of *zye* had a further effect, leading to denticles with a twisted appearance (Figure 2A). The phenotype resulting from the accumulated inactivation of *m*, *tyn*, and *zye* therefore suggests additive defects. The simultaneous inactivation of *neo*, *mey*, and *nyo* caused defects similar to individual mutations, suggesting that these proteins probably act together during denticle formation.

These data establish that denticle formation relies on the coordinated action of seven genes encoding ZPD proteins. Furthermore, the phenotypical diversity observed between mutants suggests that these proteins are involved in separate functions.

The Functional Specificity of ZPD Proteins Relies on Multiple Protein Regions

To further test the functional separation of epidermal ZPD proteins, we devised an in vivo rescue assay, based on the Gal4/UAS system that provides comparable temporal and quantitative expression of tested products. We focused on M and Tyn, representative members of the two main subclasses of ZPD in *Drosophila* (i.e., proteins with only a ZPD and those containing both ZPD and PAN extracellular motifs) (Figure 1A).

Re-expression of M under these conditions was sufficient to rescue the denticle defects observed in *m* mutant embryos (Figure 2B). It also rescued the strong reduction in size of adult wings, the phenotype at the origin of the name *miniature* (Morgan and Bridges, 1916). In addition to denticle defects in embryos, the absence of *tyn* leads to lethality at later stages. Re-expression of Tyn fully rescued *tyn* mutant defects in embryos and also restored adult viability (Figure 2B). In contrast, M overexpression was not able to suppress *tyn* phenotypes with respect to denticles and to viability. Reciprocally, Tyn failed to rescue *m* phenotypes. We then assayed the rescuing ability of Dyl and Zye that, like M, lacks PAN domains, as well as Neo and Nyo, two close epidermal relatives of Tyn (see Figure 1A). Expression of Dyl slightly modified the denticle phenotype of *m* embryos, but did not rescue adult wings, and did not improve *tyn* mutant phenotypes. Zye was also unable to compensate for the absence of *m* or *tyn*. Neo and Nyo, which comprise three PAN domains, partially restored the viability of *tyn* mutants, without, however, significantly rescuing denticles (Figure 2B). Therefore, the absence of a given ZPD protein cannot be efficiently compensated for by overexpressing a different ZPD protein, further demonstrating that they play nonredundant roles.

The fact that M and Tyn have distinct functions in the same cells offers an attractive opportunity to delineate, in vivo, the protein regions involved in their specificity. Using this genetic assay, we first tested the influence of the most prominent divergence between M and Tyn proteins (i.e., the presence of PAN domains in Tyn) (Figure 3A). Deletion of PAN domains (Tyn-[ΔPAN]) severely impaired Tyn activity, leading only to a slight modification of the denticle phenotype, and no restoration of the viability of *tyn* mutants. In addition, Tyn-[ΔPAN] was incapable of compensating for the absence of M. Reciprocally, the insertion of Tyn PAN domains within M (M-[PAN-Tyn]) resulted in a protein unable to rescue *tyn* mutants, whereas this chimerical protein retained full *m* function (Figure 3A). Thus, PAN domains are necessary for the function of Tyn, but they are not sufficient to confer *tyn* activity when added to the M protein. To test a putative contribution of the ZPD to the specificity of M and Tyn, we swapped their ZPDs (Figure 3A). Replacement of the ZPD of M with that of Tyn (M-[ZPTyn]) resulted in a protein with a reduced capacity to rescue *m* defects. However, a weak effect on the denticle phenotype of *tyn* mutants suggests that this chimera had gained some Tyn activity. In the same vein,

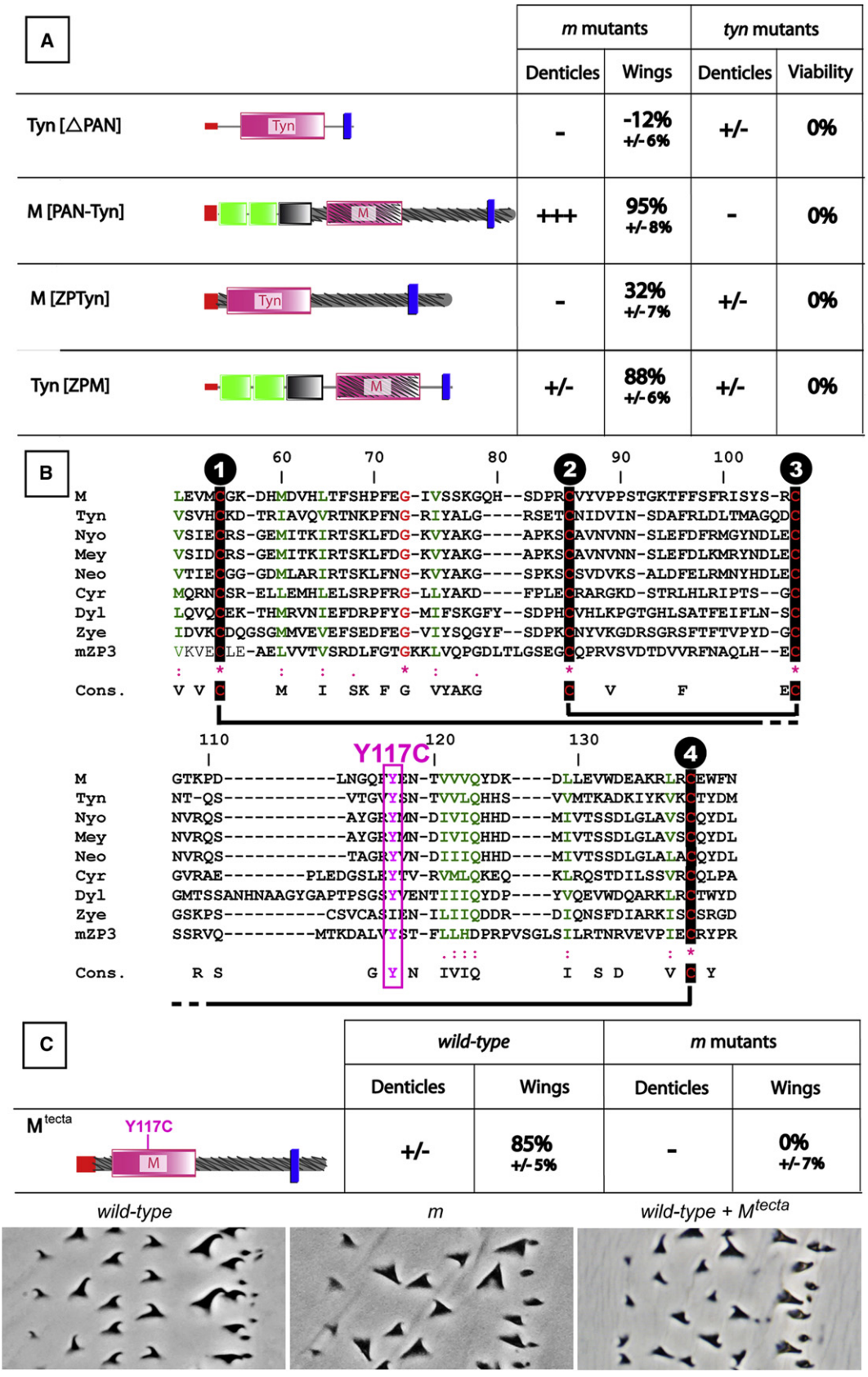
A
m mutants
tyn mutants
Denticles
Wings
Denticles
Viability
Tyn [△PAN]
Tyn
-
-12%
+/-6%
+/-
0%
M [PAN-Tyn]
M
+++
95%
+/-8%
-
0%
M [ZPTyn]
Tyn
-
32%
+/-7%
+/-
0%
Tyn [ZPM]
M
+/-
88%
+/-6%
+/-
0%
B
Y117C
Cons.
C
wild-type
m mutants
Denticles
Wings
Denticles
Wings
M tecta
Y117C
+/-
85%
+/-5%
-
0%
+/-7%
wild-type
m
wild-type + M tecta

replacing the ZPD of Tyn with that of M (Tyn-[ZPM]) provided a significant rescue of *m* loss of function in adults, albeit without rescue of denticle defects in embryos.

We further explored the function of the ZPD within the Miniature protein. The determination of a ZPD structure has recently shown the critical role of a conserved tyrosine residue for proper folding (Monne et al., 2008). A mutation substituting this tyrosine with a cysteine in human α-tectorin (TECTA) provokes dominant genetic deafness (Verhoeven et al., 1998), and its introduction into mouse ZP3 (mZP3) alters its polymerization properties (Monne et al., 2008). We generated transgenic lines encoding a Y117C mutated Miniature protein (M^{tecta}) (Figure 3B) and found that M^{tecta} was unable to rescue, even partially, the phenotypes resulting from absence of M (Figure 3C). Furthermore, increasing levels of M^{tecta} in a wild-type background progressively leads to dominant epidermal cell shape defects in both embryos and adults (Figure 3C).

Taken together, these data establish that, despite a varying degree of conservation, the different ZPD proteins coexpressed in denticle cells fulfill separate genetic functions. Functional specification of Miniature versus Trynity during evolution has relied on the divergence of multiple protein regions, including the addition of PAN domains and modification of the ZPD itself and other sequences. Finally, a mutation shown, in vitro, to affect polymerization properties of the ZPD leads to a dominant behavior in vivo, further suggesting that function of epidermal ZPD proteins in *Drosophila* involves homo- and/or heterotypic interactions.

ZPD Proteins Locally Organize the Contacts between the Apical Membrane and ECM

Having shown that several ZPD proteins play nonredundant roles in denticle formation, we then explored their cellular functions during the remodeling of epidermal cell shape.

As a first step, we analyzed the subcellular distribution of ZPD proteins during denticle formation using non-cross-reacting antibodies raised against M, Tyn, Dyl, and Zye (see Experimental Procedures). M protein was first detected at the apical surface, where it rapidly accumulated in a restricted apical region at the base of extensions (Chanut-Delalande et al., 2006). M finally became predominantly localized in the medial region of the denticle (Figure 4A), although it did not extend to the basalmost zone or to the tip of extensions. We generated a transgenic construct encoding a fully active Miniature-horseradish peroxidase (M-HRP) fusion protein (Table S2), the HRP activity of which allows direct detection by electron microscopy (Dubois et al., 2001). Confirming results by confocal analysis, M-HRP was seen to localize in denticles and accumulate in the medial region of extensions (Figure 4B). In addition, M-HRP was found associated with the aECM in the protein-rich layers of cuticle (Figure 4B). These data thus suggest that Miniature specifically modifies the local composition of the aECM surrounding the extension of the apical membrane.

While the Dyl protein appeared concomitantly with M, the apical accumulation of Tyn and Zye was slightly delayed. Similarly to M, Dyl, Tyn, and Zye were concentrated in restricted apical regions in the vicinity of growing denticles. However, Dyl was restricted to the tip of actin filaments, whereas Tyn and Zye accumulated only at the base of extensions (Figure 4A). Double staining confirmed that ZPD proteins were present in overlapping, but distinct, apical regions (Figure 4C). From the tip of the extension to the base of the apical compartment, first Dyl, then M, and, more basally, Zye and Tyn accumulated.

All together, these data therefore show that each ZPD protein is targeted to a specific apical region, revealing successive subdomains within the apical compartment of denticle cells.

ZPD Proteins Impinge on the Apical Organization of Epithelial Cells

To pursue the question of how ZPD proteins participate in the remodeling of the apical region, we undertook ultrastructural analyses of the organization of the membrane/aECM compartment.

The apical surface of smooth cells organizes actin-rich microvilli (Locke, 2001) or undulae (Moussian et al., 2007), which contact the cuticle only at their tips. In contrast, there is a continuous tight interaction between the plasma membrane and cuticle in denticles of wild-type embryos (Figures 5A–5A″). Lack of *m* disturbed this stereotyped organization, with impaired contacts between the denticle membrane and cuticle layers (Figures 5B–5B″). The absence of Dyl caused more severe defects, although again restricted to the denticle. The denticle cuticle appeared as a hollow structure, with the cell membrane lying at the bottom of the extension (Figures 5C–5C″). Since we did not detect abnormalities in the formation of actin bundles at earlier stages (Figure S2), this suggests that Dyl is required to anchor the cell membrane to the tip of the denticles. Lack of Zye also resulted in apparent abnormal gaps between the membrane and cuticle layers, generally restricted to the base of the extension (Figures 5D–5D″). Finally, the absence of Tyn caused very basal defects in membrane/cuticle interactions (Figures 5E–5E″).

Transmission electron microscopy (TEM) analysis suggested that the lack of Tyn and Zye disturbed the apical organization of denticle cells. Staining for apical determinants (Crumbs), or components of Zonula Adherens junctions (DE-cadherin), revealed that denticle cells have a smaller apical area than

Figure 3. Functional Specificity of ZPD Proteins

(A) Rescuing activities of chimeric forms of Trynity and Miniature (shaded) proteins. The three Pan-AP domains have been deleted from the Tyn protein (Tyn[ΔPAN]), or inserted at a similar position within the Miniature protein (M[PAN-Tyn]). M[ZPTyn] and Tyn[ZPM] correspond to a reciprocal exchange of the two ZPDs.

(B) Structure-based alignment of the ZP-N region of *Drosophila* M, Tyn, Nyo, Mey, Neo, Cyr, Dyl, and Zye proteins, as well as mZP3. Black boxes indicate conserved Cys residues, and lines presumptive disulfide bonds. The tyrosine residue corresponding to that substituted in human α-tectorin (Y1850C) is boxed in pink. In the Miniature protein, the introduced mutation is Y117C (M^{tecta}).

(C) Activity of M^{tecta} protein assayed in embryos (denticles) and adults (wings). M^{tecta} expression was driven by *da*-GAL4 in m^1 mutants, or in wild-type animals. In the latter, dominant defects appeared when using two copies of UAS-m^{tecta} construct, and three copies gave clear defects in all examined specimen. Pictures show denticle organization in wild-type embryos, m^1 mutant embryos, and embryos expressing M^{tecta} in an otherwise wild-type context. Adult wing size was determined as indicated in Figure 2 and Supplemental Information.

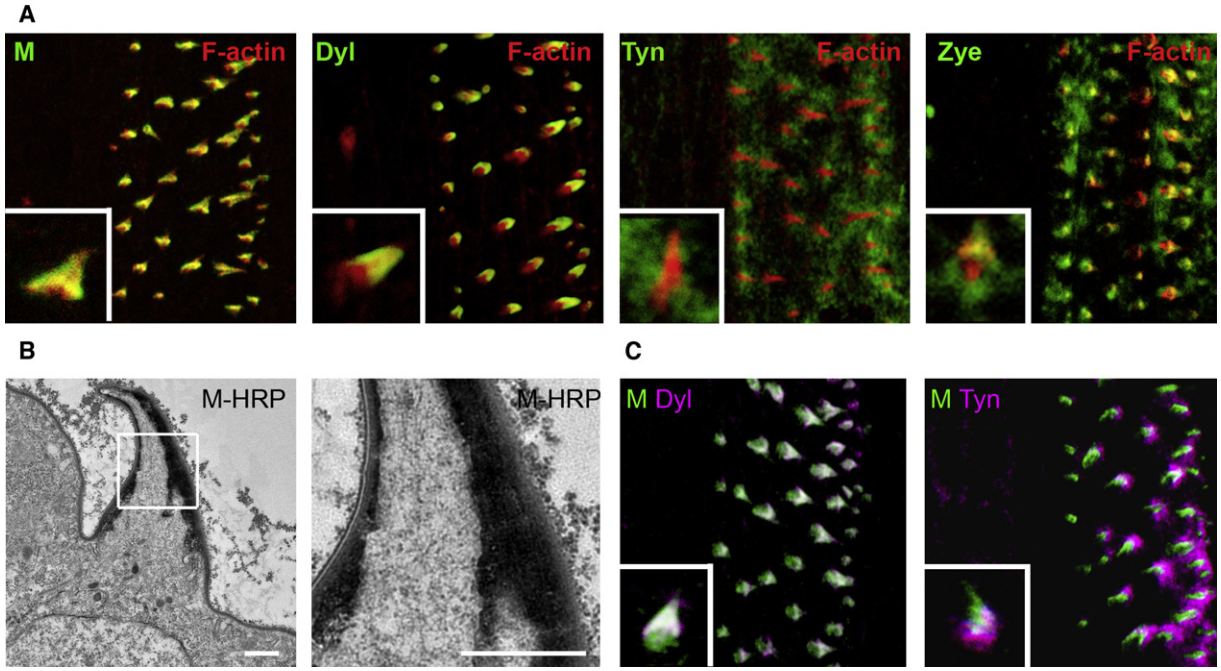

Figure 4. ZPD Proteins Localize in Specific Subapical Domains

(A) Subcellular localization of M, Dyl, Tyn, and Zye proteins in epidermal cells of stage 15 wild-type embryos (A3 or A4 segment). Actin filaments were stained by phalloidin (red) and ZPD proteins with monospecific antibodies (green). Close-up views highlight the distinct localization of ZPD proteins along the extension.

(B) TEM analysis of M-HRP localization in stage 16 embryos. HRP activity leads to a dark stain revealing M-HRP accumulation within endocuticle layers of the denticle. Scale bar, 500 nm (see also Table S2).

(C) Codetection of Miniature (green) with either Dyl or Tyn (magenta); colocalization appears in white.

smooth cells in wild-type (Figure 6A). Whereas smooth cells display a cuboidal contour, denticle cells are also markedly elongated along the dorso-ventral axis (Figures 6A and 6E). Inactivation of *tyn* or *zye* altered these typical features, leading to an enlargement of the apical surface of denticle cells, without affecting smooth cells (Figure 6). Moreover, the intensity of Crumbs staining in wild-type was significantly higher in denticle cells than in smooth cells. We noticed a similar increase in levels of DE-Cadherin (Shg) within the junctions of wild-type denticle cells (Figures 6A and 6E). The lack of *tyn* or *zye* prevented this buildup of apical complexes, which were reduced to (and often below) levels normally observed in smooth cells (Figures 6B, 6C, 6F, and 6G). In contrast, septate junctions appeared unaffected in ZPD mutants, as deduced from normal ultrastructure and distribution of Dlg or Fas3 in such embryos (Figures 6I–6L).

In sum, these data show that the different ZPD proteins are required to establish and/or maintain localized membrane/aECM contacts within restricted areas of the apical compartment. This includes the stabilization of high levels of apical protein complexes, likely to be involved in the remodeling of epidermal cells to promote the formation of apical extensions.

DISCUSSION

ZPD proteins organize various ECMs known to play important roles in adults, since mutations in ZPD genes cause infertility, deafness, or renal and vascular disorders (Jovine et al., 2005). However, our understanding of how ZPD proteins contribute to the development of embryonic tissues remains limited. Through the systematic analysis of *Drosophila* ZPD genes, we show here that a diverse subfamily of ZPD proteins contributes to remodeling the shape of embryonic epidermal cells during their differentiation. We find that each ZPD protein accumulates in, and thereby defines, a restricted apical subregion to locally modify the composition of aECM and its interaction with membrane domains.

Transcriptional Control of Epidermal Morphogenesis

The *Drosophila* embryonic epidermis provides a well-understood framework within which to address the mechanisms of changes in cell shape during development (Schock and Perrimon, 2002). The polarity of epidermal cells is progressively established throughout the period of tissue differentiation (Muller and Bossinger, 2003), and hormones subsequently control cuticle deposition (Locke, 2001; Payre, 2004). Before this, regulatory cascades define the subpopulations of cells that undergo apical shape remodeling through the control of *svb* expression (McGregor et al., 2007; Payre et al., 1999). Svb, in turn, triggers the expression of numerous factors that modify actin, membrane, and ECM organization. Svb directly controls the expression of the ZPD gene, *m* (Chanut-Delalande et al., 2006), and we show here that *m* encodes a protein addressed to the extracellular space of the cell, where it will become integrated within cuticle layers.

By means of a systematic analysis of the genomic set of ZPD genes in flies, we find that Svb actually promotes the expression

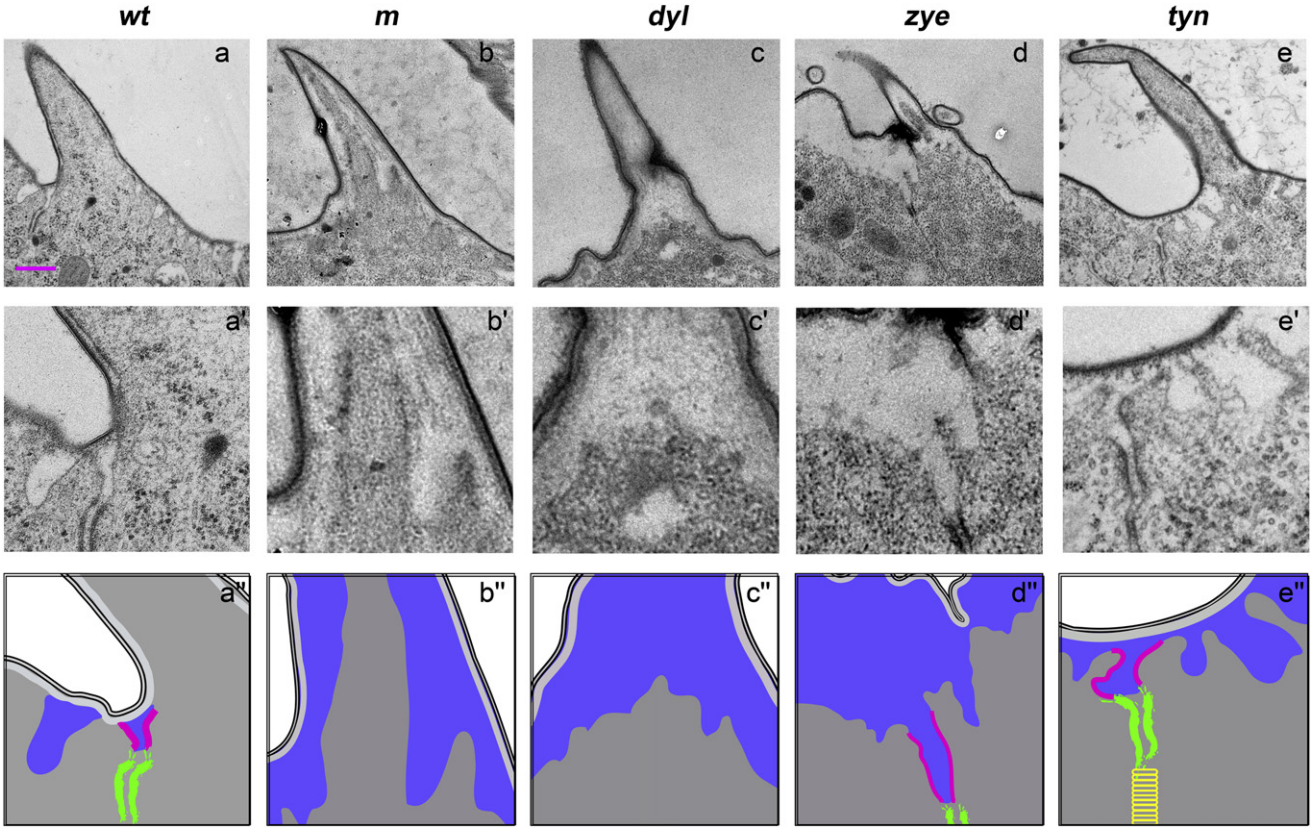

Figure 5. Ultrastructural Analysis of Denticle Defects in *m*, *dyl*, *tyn*, and *zye* Mutants

(A–E) TEM micrographs of denticle cells from wild-type, m^{1}, tyn^{PG38}, $dyl^{\Delta 26}$, and $zye^{Ey05938}$ embryos. Inactivation of *m* alters membrane/aECM contact all around the extension (B), whereas tyn^{PG38} (D) and $zye^{EY05938}$ (E) alter the base of extensions down to cell junctions. $dyl^{\Delta 26}$ mutants lack cytoplasm in the extension (C). Scale bar, 500 nm.

(A′–E′) Close-up views of images in (A)–(E).

(A″–E″) Schematic representations of close-up views, with double black lines representing the epicuticle, light gray lines endocuticle, and dark gray the cytoplasm. Pink, green, and yellow correspond to the marginal zone (MZ, also referred to as supapical region), adherens junctions (AJ), and septate junctions (SJ), respectively. Blue areas highlight regions where plasma membrane does not appear to contact cuticle layers, showing abnormal enlargement in ZPD mutants, at specific locations along the extension (see also Figure S2).

of eight ZPD genes in the precise subpopulation of epidermal cells that form trichomes. Epidermal expression of these ZPD genes generally starts at stage 14, peaks at stage 15, and becomes progressively downregulated from stage 16. This time window correlates with two major events of epidermal differentiation (i.e., the first sign of apical shape remodeling and the onset of cuticle deposition) (Moussian et al., 2006). While *m*, *dyl*, *nyo*, *neo*, *mey*, and *tyn* are transcribed in all trichome cells, *cyr* and *zye* are differentially expressed between ventral and dorsal trichome cells. We recently identified an additional ZPD gene (CG12814) in the *Drosophila* genome, and observed that *svb* triggers its expression, like that of *cyr* and *zye*, in restricted dorsoventral subsets of trichome cells (data not shown). This raises the possibility that ZPD proteins contribute to the differential shaping of trichomes observed between different cell populations. However, ZPD genes are unlikely to play a role in the row-specific shaping of denticles, because we did not detect obvious differences in their expression within each denticle belt. As shown in the case of *m* (Chanut-Delalande et al., 2006), it is possible that Svb directly controls the expression of other ZPD genes in trichome cells. Consistent with this hypothesis, genomic analysis of sequenced *Drosophilidae* species predicts the existence of conserved Ovo/Svb binding sites in noncoding regions of these *svb* downstream genes (Stark et al., 2007).

Evolutionary Diversification of ZPD Gene Functions

That Svb coregulates a set of eight closely related ZPD genes may indicate that the latter correspond to a recent evolutionary expansion and, consequently, still retain redundant functions. For example, several ZPD genes coexpressed in hypodermal cells of *Caenorhabditis elegans* embryos play at least partially redundant roles in cuticle differentiation (Muriel et al., 2003; Sapio et al., 2005; Sebastiano et al., 1991). However, several lines of evidence show that this is not the case for *Drosophila* ZPD in trichome cells. First, the individual inactivation of ZPD genes leads to characteristic denticle defects. The absence of a given ZPD gene results in a specific alteration of the denticle shape that is recognizable in both individual and combined ZPD mutants. For example, the accumulated inactivation of *m*,

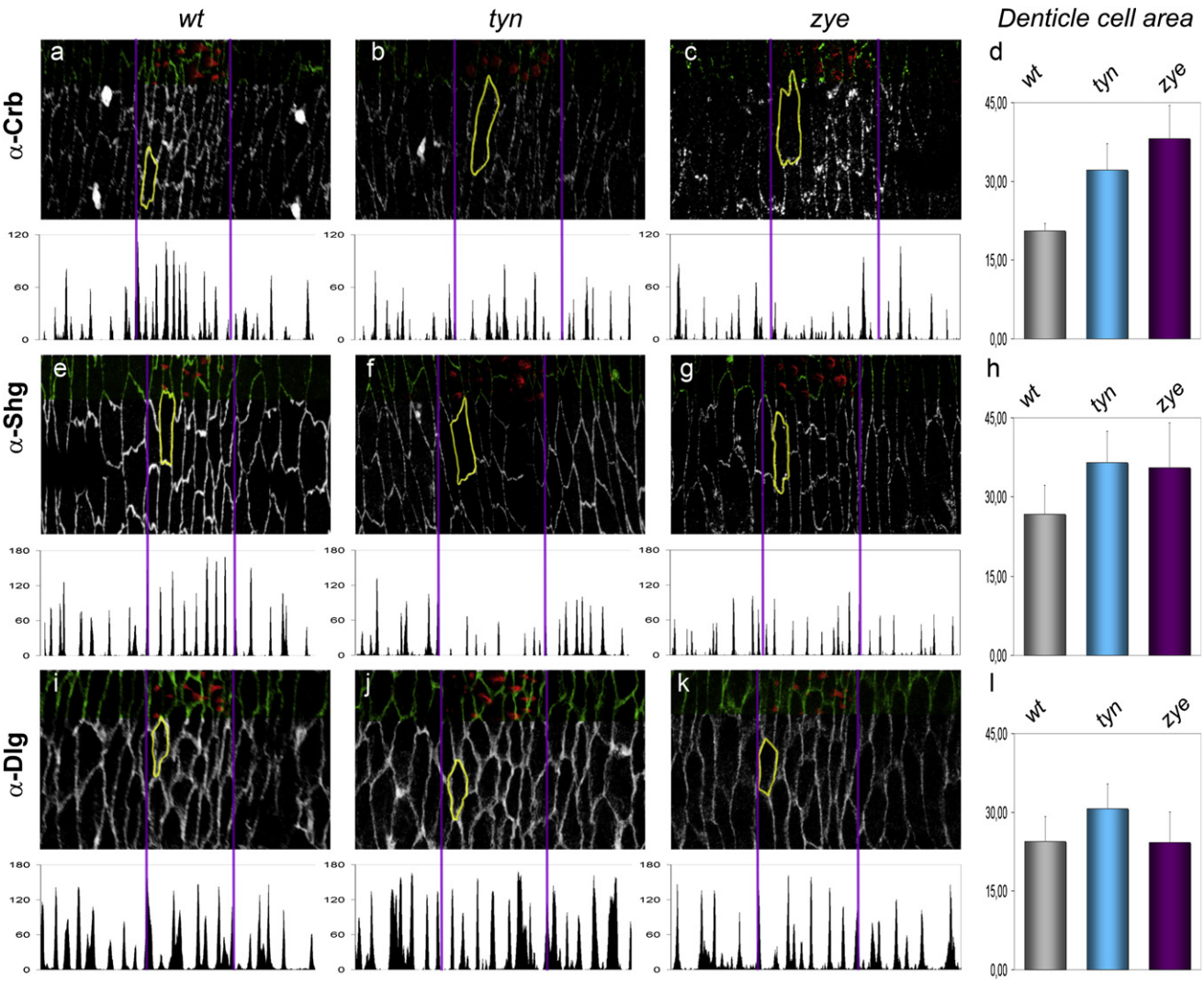

Figure 6. Disorganization of the Apical Compartment in *tyn* and *zye* Mutants

Localization (green) of Crumbs (A–D), Shotgun (E–H), and Disc-large (I–L) proteins in *wt*, tyn^{PG38}, and zye^{ex72} embryos. Apical extensions are visualized using anti-Dyl antibody (red), and magenta lines delimit denticle cells. Yellow lines outline the contour of one cell. Below confocal pictures, histograms plot the signal intensity. Crumbs levels are enhanced in *wt* denticle cells compared to naked cells (A), while signal intensity is similar in all epidermal cells in *tyn* and *zye* mutants (B and C). Shotgun is also enhanced in *wt* denticle cells (E), while diminished in *tyn* and *zye* mutants (F and G). (D, H, and L) Histograms represent the apparent area of denticle cells, as from Crb, Shg, and Dlg staining. Note the increased area of denticle cells in *tyn* and *zye* mutants when compared with wild-type (ratio, 1.6 for *tyn*/*wt*, and 1.9 for *zye*/*wt*, using the Crb staining). The mean size of embryonic epidermal cells was determined from at least 30 cells (from a minimum of five different embryos of the same genotype). Average values with SD (error bars) are represented.

tyn, and *zye* results in highly misshapen denticles, which we interpret as the additive consequences of the lack of each ZPD gene. Second, most ZPD genes diverged more than 150 million years ago, since their putative ortholog can be traced back in beetles, mosquitoes, and bees (data not shown). The only exceptions are *neo*, *nyo*, and *mey*, which probably arose from recent gene duplication in *Drosophilidae* (data not shown). Although their absence leads to a similar small-denticle phenotype, these three genes are unlikely to retain fully redundant functions in denticle formation, since their simultaneous inactivation does not increase the observed defects. Finally, our rescue experiments provide unambiguous evidence that the lack of a given ZPD gene cannot be efficiently compensated for by the overexpression of a different ZPD gene, thus demonstrating that each ZPD protein possesses a separate function for localized shaping of trichome cells.

Insights into the Functional Specificity of ZPD Proteins

One important question is, therefore, what determines the specific function of a given ZPD protein? Current models suggest a major role of the ZPD itself in the functional diversification of ZPD proteins (Wassarman, 2008). Besides the conservation of a restricted structural backbone that involves invariant cysteines, the ZPD has been the object of rapid sequence evolution

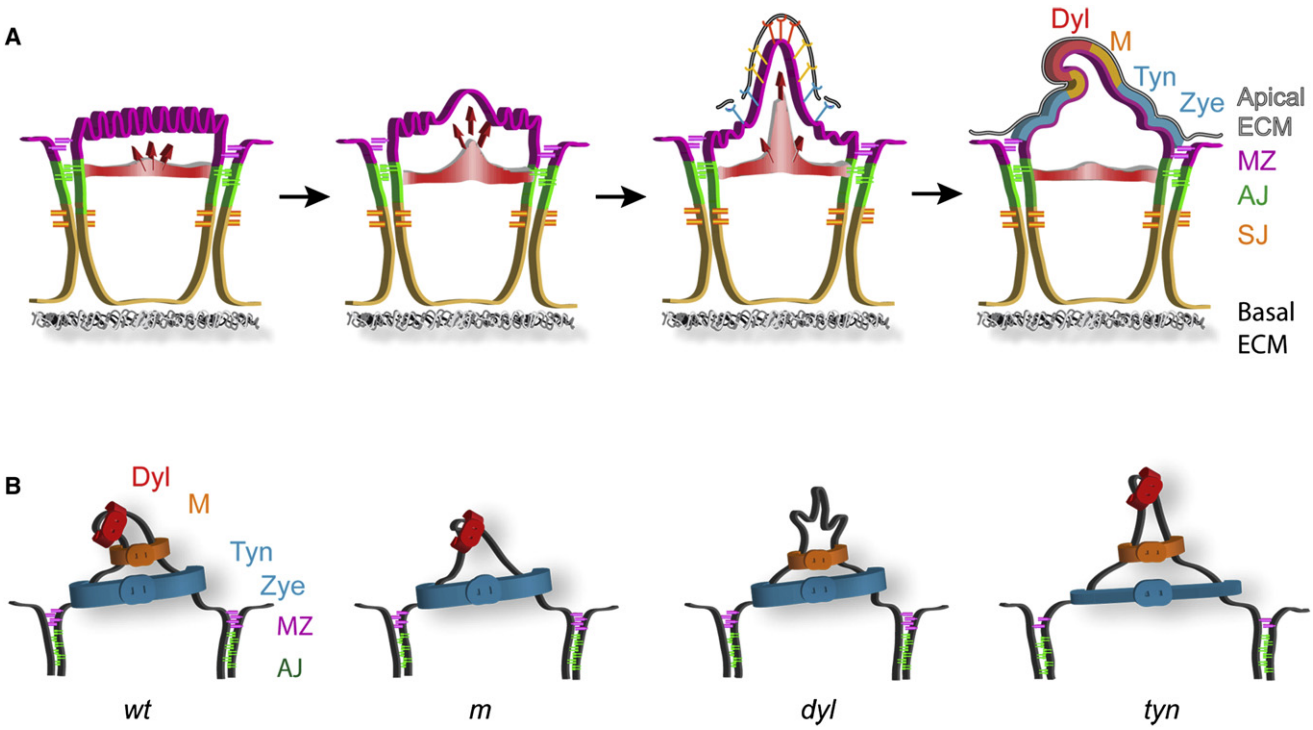

Figure 7. Model of ZPD Protein Function during Apical Cell Shape Remodeling

(A) During epidermis differentiation, the apical surface is remodeled via a thrust of actin bundles, which triggers the formation of the apical extension (denticle) beginning at stage 14. At stage 15, the localized deposition and function of ZPD proteins cause the extension to shrink, thus sculpturing and stabilizing the shape of the denticle during and after actin bundle retraction.

(B) In wild-type epidermal cells, belts, corresponding to aECM modifications mediated by each ZPD protein, shape the denticle. The loss of a given ZPD protein results in the local alteration of the aECM and/or its interaction with corresponding membrane subdomain, resulting in a specific defect of the apical cell shape.

(Figure 3B and data not shown). It has been proposed that the N-terminal half of ZPD (ZP-N) acts as a polymerization module (Jovine et al., 2006; Monne et al., 2008), while the C-terminal half (which allows alternative disulfide bond connectivity) may be a primary determinant of specificity. Our in vivo analyses support that the importance of the ZP-N is widely conserved across species, as a Y > C mutation originally identified in human TECTA (Verhoeven et al., 1998) compromises function of the *Drosophila* Miniature protein. Furthermore, mutated M^{tecta} exerts a dominant effect when expressed in wild-type animals, suggesting that, as is the case in vitro (Monne et al., 2008), this substitution within the ZP-N affects the polymerization properties of ZPD proteins. The ZPD also influences the specificity of ZPD proteins, since replacing the ZPD of Trynity by that of Miniature is sufficient to confer partial rescue of *m* defects in vivo. However, the reverse substitution does not compensate for the loss of Trynity activity, which critically relies on the presence of PAN domains. In addition, the region C terminal to the ZPD also contributes to ZPD protein specificity and, accordingly, it is strongly conserved between insect orthologs (data not shown). In the same vein, mZP3 exon 7, a region located downstream of the ZPD, is responsible for mZP3 protein specificity (Litscher et al., 2009). Our results thus show that the functional specificity of epidermal ZPD in flies is determined by multiple protein regions, and not solely by the ZPD. Extrinsic factors may also modulate the functions of ZPD proteins, since they are known to be extensively modified with N- and O-linked oligosaccharides (Jovine et al., 2005). Interestingly, several O-glycosylation enzymes are expressed in subsets of epidermal cells in *Drosophila* embryos (Tian and Ten Hagen, 2007), where they possibly regulate the activity of ZPD proteins.

Epidermal ZPD Proteins Control Polarized Changes in Cell Shape

ZPD proteins localize to distinct apical subregions of epidermal cells, in correlation with the local defects observed when a given protein is missing (Figure 7). Dyl accumulates at the tip of denticles, which are split in *dyl* mutants. M is enriched in the medial region of extensions, and *m* mutants lose the medial constriction characteristic of normal denticles. *tyn* and *zye* mutations affect the base of denticles, where the respective proteins normally accumulate. Ultrastructural analyses further show that defects in denticle shaping imply local alteration of aECM and plasma membrane, suggesting that ZPD proteins are required to organize extracellular components (and possibly their interaction with membrane), specifically in denticles. This is consistent with recent results suggesting that cuticle formation relies on highly organized protein secretion at specific locations within the apical plasma membrane (Moussian et al., 2007). Our data show that the local composition of the aECM does indeed display distinct ZPD-mediated modifications. We speculate

that a heterogeneous scaffold of ZPD proteins is necessary to induce and/or organize the local forces necessary for the correct shaping of denticles (Figure 7). A parallel can be drawn with data suggesting a mechanical role for ZPD proteins in the local remodeling of cell shape in other systems, such as elongation of pupal wing cells in *Drosophila* (Roch et al., 2003), constriction of lateral hypodermal cells in *C. elegans* (Sapio et al., 2005), and induction of columnar shape in kidney and embryonic stem cells (Takito and Al-Awqati, 2004). The ZP coat also influences the embryonic-extraembryonic axis of the mammalian blastocyst through physical constraints (Kurotaki et al., 2007), showing that ZPD proteins may be involved at multiple steps in the mechanical regulation of cell and tissue shape.

ZPD Proteins and the Polarized Organization of Epidermal Cells

The concentric distribution of ZPD proteins within the apical membrane of epidermal cells reveals a previously overlooked subcompartmentalization of the apical domain. How are these apical subcompartments defined, and how do they interact with other determinants of cell polarity? It is possible that intrinsic properties of ZPD proteins contribute to the construction of a highly ordered scaffold that organizes the apical membrane around the cell extension. Supporting this hypothesis, we observed, for example, a mislocalization of Dyl protein in *m* mutants (I.F., unpublished data). Although our genetic data are compatible with the existence of homo- and/or heterotypic interactions between epidermal ZPD proteins, extensive tests of their polymerization properties now await biochemical characterization, a challenging task due to the high level of post-translational modifications of this family of ECM proteins.

The distribution of a given ZPD protein must also rely on extrinsic factors, such as regulators of trafficking machineries, and future cellular analyses will be required to address this important issue. Routing ZPD proteins to apical subregions likely requires, as well, a proper apicobasal polarization. Unexpectedly, the most basal ZPD proteins, Tyn and Zye, are required for correct maintenance of junctional complexes and apical determinants in denticle cells. This, in turn, suggests a bidirectional interaction between ZPD proteins and junction/polarity complexes to ensure, on the one hand, proper localization of ZPD and, on the other hand, a reinforcement of junctions and apical determinants in denticle cells. Reorganization of cell junctions is critical for various changes in cell shape, such as those involved during germ band extension or mesoderm invagination (Lecuit and Lenne, 2007), and it may be involved in the stretching that occurs along the dorsoventral axis of denticle cells. In addition, deformation of the apical compartment that is mediated by actin and ECM reorganization probably requires a robust architecture of lateral structures to be translated into a coherent change in cell shape. Interestingly, Piopio and Dumpy ZPD proteins are also required for junction remodeling during trachea formation (Jazwinska et al., 2003). Likewise, the ZPD protein, Hensin/DMBT1, influences cell polarity and promotes the formation of junctional complexes (Takito and Al-Awqati, 2004), a finding that may be relevant to its deletion in various cancers (Al-Awqati, 2008).

In conclusion, these data show that local modifications of the aECM provide additional cues that influence the polarized organization of epithelial cells and are required for their morphogenesis. The specific distribution and function of ZPD proteins open future directions to explore how trafficking machineries are specified for protein delivery to apical subdomains, in intimate interaction with localized actin remodeling and fine tuning of polarity determinants and cell-cell junctions.

EXPERIMENTAL PROCEDURES

Fly Strains

UAS-m, UAS-tyn, UAS-dyl, UAS-neo, UAS-tyn[ΔPAN], UAS-m[PAN-tyn], UAS-m[ZPtyn], UAS-tyn[ZPm], UAS-mHRP, and UAS-m^{tecta} transgenic lines were generated using P-element transformation. Unless specified, other stocks were obtained from the Bloomington stock center: m^{1}, tyn^{PG38} (P[GawB]SP71^{PG38} (Bourbon et al., 2002), $zye^{EY05938}$ (P[EPgy2]^{EY05938}), svb^{1}, svb^{1}, btd^{1}, and *da*-GAL4. We generated null alleles for *tyn* and *zye* and induced the small deficiencies, Δdyl^{26}, Δneo^{36}, Δnyo^{32}, Δmey^{13}; Δnyo-*mey*, using the procedure described by Parks et al. (2004) (see Figure S1). A strain that combined Δnyo-*mey* and Δneo^{36} was obtained by meiotic recombination. Each stock was confirmed by molecular characterization, and mutant chromosomes were kept over balancers carrying Kr-Gal4; UAS-GFP transgenes.

Molecular Procedures

UAS constructs are pUAST derivatives generated from cDNAs for *m*, *tyn*, *dyl*, *neo*, *nyo*, and *cyr* (DGRC consortium) or using PCR-amplified ORF from BAC-R02B14 for *zye*. Plasmids encoding modified ZPD proteins and HRP fusions were generated using PCR and QuikChange XL site-directed mutagenesis (Stratagene). All constructs were verified by sequencing (see Supplemental Information for detailed procedures).

Antibody Production and Staining

DNA fragments corresponding to protein regions, S_{266}-T_{358} for Tyn, and P_{354}-G_{497} for Dyl, were cloned into pGEX6p1 and GST-fusion proteins, purified according to the manufacturer's specification (GE Healthcare), were used for immunizing rats and rabbits (Agrobio). For Zye, rabbits were immunized with the synthetic peptide, EFDDSSPRLTRDTSLC (Eurogentec), and antibodies were affinity purified. In each case, antibody specificity was attested by the lack of signal observed in embryos lacking the corresponding protein. Staining was performed according to Chanut-Delalande et al. (2006), with anti-M (Roch et al., 2003) at 1/200, anti-Dyl at 1/300, anti-Tyn at 1/300, anti-Zye 1/20, α-crb (Cq4, 1/500), α-Shg (DCAD2, 1/50), α-Dlg (4F3, 1/100) (the latter three from DSHB, Iowa), AlexaFluor-488 or AlexaFluor-546 secondary antibodies at 1/1000 (Molecular Probes), and TRITC-phalloidin (Sigma). Embryos were imaged with a Leica TSP2 confocal microscope.

In Situ Hybridization

Dig- or biotin-labeled antisense RNA probes were synthesized from cDNA or genomic fragments and used for in situ hybridization experiments, as described previously (Chanut-Delalande et al., 2006). Fluorescent in situ hybridizations were processed using TSA following the manufacturer's specification (Molecular Probes).

Electron Microscopy

Live mutant embryos were hand selected under a stereomicroscope equipped for epifluorescence. Stage-16 embryos were fixed for 15 min in heptane saturated with glutaraldehyde, hand devitellinized, washed in water, and dehydrated through ethanol series. Following critical-point drying (CPD750 Emscope), they were sputtered with a 2.9 nm platinum coat (JEOL JFC2300HR) and examined with a JEOL JSM6700F scanning electron microscope. For TEM, embryos were fixed and devitellinized as above and, for M-HRP detection, were stained in DAB solution. Following postfixation for 1 hr in 1% osmium tetroxide and dehydration, samples were embedded in Epon. Sections were stained with uranyl acetate and photographed with a JEOL 2100CRP200 keV.

SUPPLEMENTAL INFORMATION

Supplemental Information includes two figures, two tables, and Supplemental Experimental Procedures and can be found with this article online at doi:10.1016/j.devcel.2009.11.009.

ACKNOWLEDGMENTS

We are grateful to the Bloomington *Drosophila* Stock Center, Developmental Studies Hybridoma Bank, and the *Drosophila* Genomic Resource Center for providing us with flies, antibodies, and molecular clones. We are indebted to A. Leru, B. Ronsin, S. Balor, and N. Benmeradi (Toulouse RIO Imaging), M. Düggelin and U. Sauder (Zentrum Mikroskopie der Universität Basel), I. Fourquaux and B. Payre (CMEAB), and S. Leblond (TEMSCAN) for their help with microscopy, and to P. Valenti for excellent technical assistance. We also thank J. Smith, P. Blader, and A. Vincent for critical reading of the manuscript. This work was supported by grants from the Association pour la Recherche contre le Cancer (no. 3832, no. 1111, and a fellowship to I.F.) and the Fondation pour la Recherche Médicale (programme équipe 2005). The authors declare no conflict of interest. I.F., H.C.D., F.P., and S.P. conceived and designed the experiments. I.F., H.C.D., Y.L., P.F., and S.P. performed the experiments and are listed according to their respective contributions. I.F., H.C.D., P.F., S.P., and F.P. wrote the paper. L.W. and M.A. contributed reagents and analytical tools.

Received: April 8, 2009
Revised: October 6, 2009
Accepted: November 13, 2009
Published: January 19, 2010

REFERENCES

Al-Awqati, Q. (2008). 2007 Homer W. Smith Award: control of terminal differentiation in epithelia. J. Am. Soc. Nephrol. *19*, 443–449.

Andrew, D.J., and Baker, B.S. (2008). Expression of the *Drosophila* secreted cuticle protein 73 (Dsc73) requires Shavenbaby. Dev. Dyn. *237*, 1198–1206.

Andrews, J., Garcia-Estefania, D., Delon, I., Lu, J., Mevel-Ninio, M., Spierer, A., Payre, F., Pauli, D., and Oliver, B. (2000). OVO transcription factors function antagonistically in the *Drosophila* female germline. Development *127*, 881–892.

Bourbon, H.M., Gonzy-Treboul, G., Peronnet, F., Alin, M.F., Ardourel, C., Benassayag, C., Cribbs, D., Deutsch, J., Ferrer, P., Haenlin, M., et al. (2002). A P-insertion screen identifying novel X-linked essential genes in *Drosophila*. Mech. Dev. *110*, 71–83.

Chanut-Delalande, H., Fernandes, I., Roch, F., Payre, F., and Plaza, S. (2006). Shavenbaby couples patterning to epidermal cell shape control. PLoS Biol. *4*, e290. 10.1371/journal.pbio.0040290.

Delon, I., Chanut-Delalande, H., and Payre, F. (2003). The Ovo/Shavenbaby transcription factor specifies actin remodelling during epidermal differentiation in *Drosophila*. Mech. Dev. *120*, 747–758.

Delon, I., and Payre, F. (2004). Evolution of larval morphology in flies: get in shape with shavenbaby. Trends Genet. *20*, 305–313.

Dubois, L., Lecourtois, M., Alexandre, C., Hirst, E., and Vincent, J.P. (2001). Regulated endocytic routing modulates Wingless signaling in *Drosophila* embryos. Cell *105*, 613–624.

Jazwinska, A., and Affolter, M. (2004). A family of genes encoding zona pellucida (ZP) domain proteins is expressed in various epithelial tissues during *Drosophila* embryogenesis. Gene Expr. Patterns *4*, 413–421.

Jazwinska, A., Ribeiro, C., and Affolter, M. (2003). Epithelial tube morphogenesis during *Drosophila* tracheal development requires Piopio, a luminal ZP protein. Nat. Cell Biol. *5*, 895–901.

Jovine, L., Qi, H., Williams, Z., Litscher, E., and Wassarman, P.M. (2002). The ZP domain is a conserved module for polymerization of extracellular proteins. Nat. Cell Biol. *4*, 457–461.

Jovine, L., Darie, C.C., Litscher, E.S., and Wassarman, P.M. (2005). Zona pellucida domain proteins. Annu. Rev. Biochem. *74*, 83–114.

Jovine, L., Janssen, W.G., Litscher, E.S., and Wassarman, P.M. (2006). The PLAC1-homology region of the ZP domain is sufficient for protein polymerisation. BMC Biochem. *7*, 11. 10.1186/1471-2091-7-11.

Kurotaki, Y., Hatta, K., Nakao, K., Nabeshima, Y., and Fujimori, T. (2007). Blastocyst axis is specified independently of early cell lineage but aligns with the ZP shape. Science *316*, 719–723.

Lecuit, T., and Lenne, P.F. (2007). Cell surface mechanics and the control of cell shape, tissue patterns and morphogenesis. Nat. Rev. Mol. Cell Biol. *8*, 633–644.

Litscher, E.S., Williams, Z., and Wassarman, P.M. (2009). Zona pellucida glycoprotein ZP3 and fertilization in mammals. Mol. Reprod. Dev. *76*, 933–941.

Locke, M. (2001). The Wigglesworth Lecture: insects for studying fundamental problems in biology. J. Insect Physiol. *47*, 495–507.

McGregor, A.P., Orgogozo, V., Delon, I., Zanet, J., Srinivasan, D.G., Payre, F., and Stern, D.L. (2007). Morphological evolution through multiple *cis*-regulatory mutations at a single gene. Nature *448*, 587–590.

Mellman, I., and Nelson, W.J. (2008). Coordinated protein sorting, targeting and distribution in polarized cells. Nat. Rev. Mol. Cell Biol. *9*, 833–845.

Monne, M., Han, L., Schwend, T., Burendahl, S., and Jovine, L. (2008). Crystal structure of the ZP-N domain of ZP3 reveals the core fold of animal egg coats. Nature *456*, 653–657.

Morgan, T.H., and Bridges, C.B. (1916). Sex-Linked Inheritance in *Drosophila* (Washington, DC: Carnegie Institution of Washington), pp. 1–88.

Moussian, B., Seifarth, C., Muller, U., Berger, J., and Schwarz, H. (2006). Cuticle differentiation during *Drosophila* embryogenesis. Arthropod Struct. Dev. *35*, 137–152.

Moussian, B., Veerkamp, J., Muller, U., and Schwarz, H. (2007). Assembly of the *Drosophila* larval exoskeleton requires controlled secretion and shaping of the apical plasma membrane. Matrix Biol. *26*, 337–347.

Muller, H.A., and Bossinger, O. (2003). Molecular networks controlling epithelial cell polarity in development. Mech. Dev. *120*, 1231–1256.

Muriel, J.M., Brannan, M., Taylor, K., Johnstone, I.L., Lithgow, G.J., and Tuckwell, D. (2003). M142.2 (cut-6), a novel *Caenorhabditis elegans* matrix gene important for dauer body shape. Dev. Biol. *260*, 339–351.

Parks, A.L., Cook, K.R., Belvin, M., Dompe, N.A., Fawcett, R., Huppert, K., Tan, L.R., Winter, C.G., Bogart, K.P., Deal, J.E., et al. (2004). Systematic generation of high-resolution deletion coverage of the *Drosophila melanogaster* genome. Nat. Genet. *36*, 288–292.

Payre, F. (2004). Genetic control of epidermis differentiation in *Drosophila*. Int. J. Dev. Biol. *48*, 207–215.

Payre, F., Vincent, A., and Carreno, S. (1999). ovo/svb integrates Wingless and DER pathways to control epidermis differentiation. Nature *400*, 271–275.

Roch, F., Alonso, C.R., and Akam, M. (2003). *Drosophila* miniature and dusky encode ZP proteins required for cytoskeletal reorganisation during wing morphogenesis. J. Cell Sci. *116*, 1199–1207.

Sapio, M.R., Hilliard, M.A., Cermola, M., Favre, R., and Bazzicalupo, P. (2005). The zona pellucida domain containing proteins, CUT-1, CUT-3 and CUT-5, play essential roles in the development of the larval alae in *Caenorhabditis elegans*. Dev. Biol. *282*, 231–245.

Schock, F., and Perrimon, N. (2002). Molecular mechanisms of epithelial morphogenesis. Annu. Rev. Cell Dev. Biol. *18*, 463–493.

Sebastiano, M., Lassandro, F., and Bazzicalupo, P. (1991). cut-1 a *Caenorhabditis elegans* gene coding for a dauer-specific noncollagenous component of the cuticle. Dev. Biol. *146*, 519–530.

Stark, A., Lin, M.F., Kheradpour, P., Pedersen, J.S., Parts, L., Carlson, J.W., Crosby, M.A., Rasmussen, M.D., Roy, S., Deoras, A.N., et al. (2007). Discovery of functional elements in 12 *Drosophila* genomes using evolutionary signatures. Nature *450*, 219–232.

Sucena, E., Delon, I., Jones, I., Payre, F., and Stern, D.L. (2003). Regulatory evolution of shavenbaby/ovo underlies multiple cases of morphological parallelism. Nature *424*, 935–938.

Takito, J., and Al-Awqati, Q. (2004). Conversion of ES cells to columnar epithelia by hensin and to squamous epithelia by laminin. J. Cell Biol. *166*, 1093–1102.

Tian, E., and Ten Hagen, K.G. (2007). O-linked glycan expression during *Drosophila* development. Glycobiology *17*, 820–827.

Tordai, H., Banyai, L., and Patthy, L. (1999). The PAN module: the N-terminal domains of plasminogen and hepatocyte growth factor are homologous with the apple domains of the prekallikrein family and with a novel domain found in numerous nematode proteins. FEBS Lett. *461*, 63–67.

Verhoeven, K., Van Laer, L., Kirschhofer, K., Legan, P.K., Hughes, D.C., Schatteman, I., Verstreken, M., Van Hauwe, P., Coucke, P., Chen, A., et al. (1998). Mutations in the human alpha-tectorin gene cause autosomal dominant non-syndromic hearing impairment. Nat. Genet. *19*, 60–62.

Wassarman, P.M. (2008). Zona pellucida glycoproteins. J. Biol. Chem. *283*, 24285–24289.

Wodarz, A., and Nathke, I. (2007). Cell polarity in development and cancer. Nat. Cell Biol. *9*, 1016–1024.